Physica D 67 (1993) 327–346
North-Holland

SDI: 0167-2789(93)E0186-F

PHYSICA D

Rigorous chaos verification in discrete dynamical systems

Arnold Neumaier [a,1] and Thomas Rage [b,2]

[a] *Institut für Angewandte Mathematik, Albert-Ludwigs-Universität Freiburg, Hermann-Herder-Straße 10, W-79104 Freiburg i. Br., Federal Republic of Germany*

[b] *Fakultät für Physik, Albert-Ludwigs-Universität Freiburg, Hermann-Herder-Straße 3, W-79104 Freiburg i. Br., Federal Republic of Germany and Department of Physics, University of Oslo, Postbox 1048 Blindern, N-0314 Oslo, Norway*

Received 1 September 1992
Revised manuscript received 15 March 1993
Accepted 15 March 1993
Communicated by F.H. Busse

In this paper we show how interval analysis can be used to calculate rigorously valid enclosures of transversal homoclinic points in discrete dynamical systems. The existence of such points guarantees that a Smale horseshoe is embedded in the mapping which therefore is chaotic. We take special interest in the 2-dimensional case and describe a method to obtain a computer-assisted proof of chaos for these systems. Numerical results are presented for the standard map.

1. Introduction

There is quite a lot of attention directed towards the concept of chaos in deterministic dynamical systems and much effort is put both into the understanding of the observed phenomena and into its proof in real systems.

For discrete dynamical systems, an illuminative chaos criterion is the existence of transversal homoclinic points created by transversal crossings of the stable and unstable manifolds of a hyperbolic fixed point. We give a brief overview of this topic in section 2.

To prove this chaos criterion for a given mapping, we will study the system numerically on a computer. But using e.g. double-precision arithmetic in our calculations would contaminate our data with statistical noise produced by rounding and truncation errors, which makes them useless for *rigorously* valid mathematical statements.

There has been recent interesting work [6,7] on establishing rigorously the existence of true *trajectories* close to ('shadowing') pseudo-orbits computed by finite-precision arithmetic, these techniques appear too weak to establish the location of *invariant manifolds*, let alone of their transversal intersection. *Nonexistence* of certain kinds of invariant manifolds – rotational invariant circles – has also

[1] E-mail address: neum@indi4.mathematik.uni-freiburg.de.
[2] E-mail address: trage@fys.uio.no.

Elsevier Science Publishers B.V.

been shown rigorously; see MacKay and Percival [15]. However, both techniques seem to be – at least at present – restricted to 2-dimensional mappings.

We therefore adopt the methods of interval analysis, i.e. our mathematical statements and numerical calculations are based on rigorous interval enclosures of all quantities of interest. We state in sections 3 the appropriate theorems to give rigorous proof of transversal homoclinic points, and prove them in section 6. The methods apply in principle (i.e., assuming the availability of sufficiently accurate arithmetic and sufficient computer time) to homoclinic points of manifolds corresponding to arbitrary hyperbolic fixed points whose Jacobian has real, simple eigenvalues only. (For other rigorous methods which allow in special situations a chaos proof without the help of a computer, see Marotto [12], Matsumoto et al. [13], Aubry and Abramovici [1], and the references in Battelli and Palmer [2].)

In section 4 we discuss the application of the formulae for 2-dimensional mappings and put forward some problems that occur in practice. Finally, in section 5, we present some of the results of the application of the method to the standard map.

All of our interval calculations were performed on an IBM 3090 computer where the programming language ACRITH-XSC was available to us. This extension of FORTRAN 77 provides the possibility of working with intervals as with real numbers. In particular, the interval versions of all operations and elementary functions are implemented. Additionally, ACRITH-XSC contains a software library that offers some very helpful problem solving routines for interval calculations.

2. Transversal homoclinic points and chaos

We briefly review a criterion for deterministic chaos in discrete dynamical systems. More extensive discussions can be found in Tabor [19]. The relation between this phenomenon and transport in phase space has been studied by Wiggins [20]. For simplicity, we restrict ourselves to 2-dimensional, invertible mappings. The main features do not change in the higher-dimensional case, but only become less obvious. In the same way, the invertibility of the mapping is not necessary but simplifies the formulation.

So, let $F\colon \Omega \subset \mathbb{R}^2 \to \mathbb{R}^2$ be a discrete diffeomorphism with inverse $F^{-1}\colon F(\Omega) \to \Omega$. Additionally, let x^* be a fixed point of F such that $F(x^*) = x^*$.

To determine the 'signature' of x^* (i.e. the effect of F on points close to x^*), one calculates the eigenvalues λ_i and eigenvectors e_i, $i = 1, 2$ of the Jacobian matrix $J = F'(x^*)$ which consists of the partial derivatives of F at the fixed point. x^* is called *hyperbolic*, if J has two real, nonzero eigenvalues such that $|\lambda_1| < 1 < |\lambda_2|$. If x^* is hyperbolic, a sequence (x_n) of points $x_n = J^n e_1 = \lambda_1^n e_1$ decays exponentially to zero and a sequence (x_n) with $x_n = J^n e_2 = \lambda_2^n e_2$ increases exponentially to infinity. Accordingly one refers to e_1 as the *stable* (e^s) and to e_2 as the *unstable* eigenvector e^u of J.

Corresponding to this, the *stable and unstable sets* W^s and W^u of a hyperbolic fixed point x^* are defined by

$$W^s := \{x \in \Omega \mid \lim_{n\to\infty} F^n(x) = x^*\} \quad \text{and} \quad W^u := \{x \in \Omega \mid \lim_{n\to\infty} F^{-n}(x) = x^*\},$$

respectively. These sets are invariant under F and F^{-1} and – as F is a diffeomorphism – are manifolds of Ω (cf. Smale [18]). As x^* belongs both to the stable and unstable manifold, W^s and W^u cross in x^*; their tangents just being the stable and unstable eigenvectors of J.

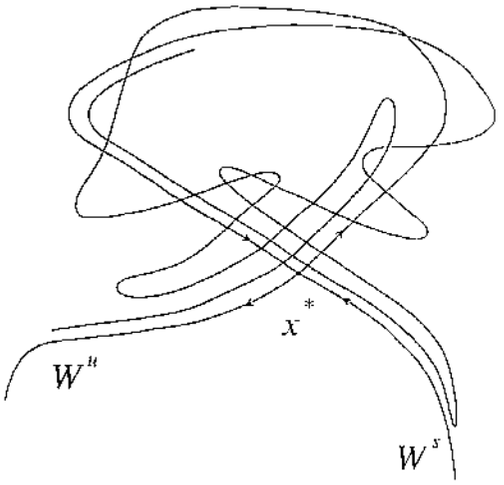

Fig. 1. Transversal homoclinic points correspond to a homoclinic tangle.

But x^* does not need to be the only crossing of W^s and W^u, and any point $x_h \neq x^*$ being an element both of W^s and W^u is called *homoclinic*. If W^s and W^u cross transversally in x_h, x_h is called *transversal homoclinic point*.

Note that once there is a transversal homoclinic point x_h, there are infinitely many of them: With W^s and W^u being invariant sets, $F^n(x_h)$ and $F^{-n}(x_h)$ are transversal homoclinic points for all $n \in \mathbb{N}$. Therefore W^s and W^u must intersect repeatedly, forming a complicated network as it is shown schematically in fig. 1. One refers to this structure as a *homoclinic tangle*, where W^s and W^u form so called *tendrils*. Smale [18] showed that in every neighbourhood of a transversal homoclinic point there is a periodic point x_p such that $F^m(x_p) = x_p$ for some $m \in \mathbb{N}$. In other words: Even arbitrarily close to a transversal homoclinic point, we find a periodic point which produces an orbit completely different to the one of the transversal homoclinic point. This "Sensitive Dependence on the Initial Condition" is a typical feature of deterministic chaos.

An even stronger justification for calling dynamical systems containing a transversal homoclinic point chaotic relies on the following observation: In the neighbourhood of every transversal homoclinic point there is an invariant Cantor set Λ such that the restriction of F to Λ is topologically equivalent to a Bernoulli-shift, i.e. a *mixing* system (cf. Smale [5]).

3. Interval methods

In the following, we shall freely use methods and terminology of interval analysis, as exposed in Neumaier [16]. In particular we write $\mathbb{IR}$, $\mathbb{IR}^n$ and $\mathbb{IR}^{m\times n}$ for the set of all compact intervals, interval vectors of length n and interval $m \times n$-matrices respectively. A vector $x = [\underline{x}, \overline{x}] \in \mathbb{IR}^n$ with components $x_k = [\underline{x}_k, \overline{x}_k] \in \mathbb{IR}$ is considered as a box consisting of all $\tilde{x} \in \mathbb{R}^n$ such that $\underline{x} \leqslant \tilde{x} \leqslant \overline{x}$, where inequalities are understood componentwise. Midpoint $\check{x}$ and radius $\mathrm{rad}(x)$ of $x \in \mathbb{IR}^n$ are given by $\check{x} = (\overline{x} + \underline{x})/2$ and $\mathrm{rad}(x) = (\overline{x} - \underline{x})/2 \geqslant 0$.

Before we explain the details of our method to prove the existence of transversal homoclinic points, let us introduce the term 'linear enclosure', which lies at the heart of our constructions:

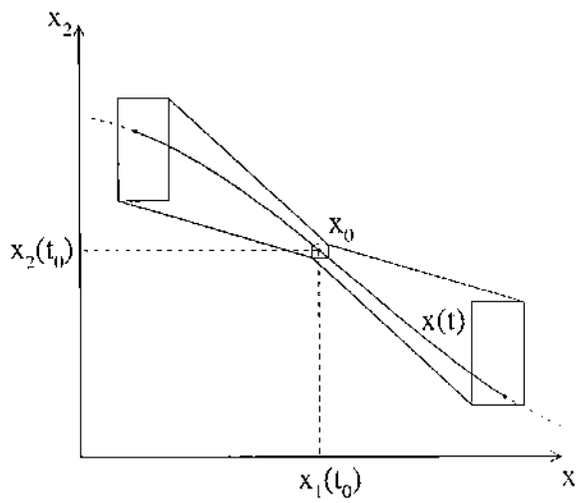

Fig. 2. Representation of a linear enclosure of a 2-dimensional curve $x(t)$.

Consider a p-dimensional manifold $x(t) \subset \mathbb{R}^N$ parametrized by the parameter $t \in \mathbb{R}^p$. A *linear enclosure* is a local enclosure of $x(t)$ defined by the four quantities $t_0, \delta \in \mathbb{R}^p$, $x_0 \in \mathbb{IR}^N$ and $K \in \mathbb{IR}^{N\times p}$ such that

$$x(t_0) \in x_0, \quad x(t) - x(s) \in K(t-s), \qquad \text{for all } t,s \in [t_0-\delta, t_0+\delta]. \tag{1}$$

It follows from (1) that

$$x(t) \in x_0 + K(t-t_0) \quad \text{for } t \in [t_0-\delta, t_0+\delta].$$

However, (1) is much stronger as it postulates an affine invariant form of Lipschitz-continuity of $x(t)$ which allows to extract angle information at each point of $x(t)$.

For curves in 2 dimensions ($N = 2, p = 1$), a linear enclosure can be visualized graphically and implies that the curve $x(t)$ lies for $t \in [t_0, t_0+\delta]$ in the region defined by the convex hull of the boxes x_0 and $x_0 + K\delta$, and for $t \in [t_0-\delta, t_0]$ in the region defined by the convex hull of the boxes x_0 and $x_0 - K\delta$. Thus a linear enclosure has the shape of a bow tie (cf. fig. 2).

Given a linear enclosure, we obtain 'pieces of the linear enclosure' (which as well are linear enclosures) just by restricting t to any set $[\underline{t}, \overline{t}] \subset [t_0-\delta, t_0+\delta]$.

Using linear enclosures, one can use theorems 1–3 below to construct a rigorous enclosure of a transversal homoclinic point of a map F by performing the following four steps:

– Calculate a rigorous enclosure x^* of a hyperbolic fixed point of F.

– Calculate linear enclosures of W^u and W^s in regions Ω^u and Ω^s that contain x^* (with the help of theorem 1).

– Take appropriate pieces of these linear enclosures and iterate them (with the help of theorem 2) to obtain linear enclosures of W^u and W^s in the neighbourhood of a (suspected) transversal homoclinic point.

– With the help of theorem 3, check for the transversal intersection of these iterated linear enclosures. Should this situation arise, calculate an interval enclosure x_h that contains the point of transversal intersection.

We will now state the theorems that are necessary to perform the last three steps.

3.1. An existence theorem

In Chapter X.5 of his well-known book on ordinary differential equations, Hartman [9] proves a local existence theorem for stable manifolds of nonlinear mappings F defined in a neighbourhood Ω of a fixed point x^*. In this section we formulate a semilocal version of this theorem. In contrast to a local result which implies the existence of *sufficiently small* neighbourhoods with certain properties, a semilocal result is stronger in that it gives *verifiable* conditions under which *specified* neighbourhoods have these properties. The precise statement of the theorem is rather complex since all conditions have to be stated in a computer-implementable form.

Theorem 1. Let the mapping $F : \Omega \subseteq \mathbb{R}^n \to \mathbb{R}^n$ be Lipschitz continuous with fixed point $x^* \in \Omega$, and let $A \in \mathbb{IR}^{n\times n}$ be an interval matrix such that

$$F(y) - F(x) \in A(y - x) \quad \text{for all } x, y \in \Omega. \tag{2}$$

For some nonsingular matrix $Q \in \mathbb{R}^{n\times n}$, let

$$Q^{-1}(AQ) = \begin{pmatrix} B_{11} & B_{12} \\ B_{21} & B_{22} \end{pmatrix} \tag{3}$$

with interval matrices B_{11}, B_{12}, B_{21} and B_{22} of sizes $p \times p$, $p \times q$, $q \times p$ and $q \times q$, respectively, where $p + q = n$. For some nonsingular matrix $C \in \mathbb{R}^{q\times q}$ and some interval matrix $L \in \mathbb{IR}^{q\times p}$, put

$$D := I + C(LB_{12} - B_{22}), \tag{4}$$

$$E := C(LB_{11} - B_{21}), \tag{5}$$

$$K := Q\begin{pmatrix} I \\ L \end{pmatrix}, \tag{6}$$

$$M := B_{11} + B_{12}L. \tag{7}$$

If the closure conditions

$$\|D\|_p + \|C\|_q \|M\|_p \leqslant \beta < 1, \tag{8}$$

$$DL + E \subseteq L \tag{9}$$

hold for suitable norms $\|.\|_p$ in $\mathbb{R}^p$ and $\|.\|_q$ in $\mathbb{R}^q$, then, for any subset Σ of $\mathbb{R}^p$ with

$$0 \in \Sigma, Mt \subseteq \Sigma \quad \text{for } t \in \Sigma, \tag{10}$$

$$x^* + Kt \subseteq \Omega \quad \text{for } t \in \Sigma, \tag{11}$$

there are unique Lipschitz continuous functions $x : \Sigma \to \Omega$, $g : \Sigma \to \mathbb{R}^q$, and $\sigma : \Sigma \to \Sigma$ such that

$$F(x(t)) = x(\sigma(t)) \quad \text{for } t \in \Sigma, \tag{12}$$

$$x(t) = x^* + Q\begin{pmatrix} t \\ g(t) \end{pmatrix} \quad \text{for } t \in \Sigma, \tag{13}$$

$$x(0) = x^*, x(s) - x(t) \in K(s-t) \quad \text{for } s,t \in \Sigma, \tag{14}$$

$$g(0) = 0, g(s) - g(t) \in L(s-t) \quad \text{for } s,t \in \Sigma, \tag{15}$$

$$\sigma(0) = 0, \sigma(s) - \sigma(t) \in M(s-t) \quad \text{for } s,t \in \Sigma. \tag{16}$$

We comment on the meaning of the various terms, and defer the proof of this theorem (which elucidates the origin of the various conditions needed) to section 6.

1. F is the mapping defining the dynamical system under investigation. Equation (12) states that $\{x(t) | t \in \Sigma\}$ is part of an invariant manifold of F. (13) gives an explicit parametrization of x with the help of a function g that contains the nonlinearities and is small near the fixed point.

2. Equations (2) and (14) - (16) are strong versions of Lipschitz continuity ($\|A\|$, $\|K\|$, $\|L\|$ and $\|M\|$ are Lipschitz constants). In typical applications, F is continuously differentiable in Ω, Ω is a box, and $A = F'(\Omega)$ is obtained as an interval enclosure of the Jacobian $F'(\xi)$, $\xi \in \Omega$. (2) holds then by a version of the mean value theorem. A useful trial value for L is given in 5 below.

3. If Ω is narrow enough, we find that $A \approx F'(x^*) = J$, the matrix which determines the signature of the fixed point. Suppose, J has p eigenvalues λ_i with $|\lambda_i| \leqslant \lambda < 1$ and q eigenvalues λ_j with $|\lambda_j| \geqslant \lambda' > 1$. If $p + q = n$ there is a p-dimensional stable manifold, part of which is to be enclosed. (We assume that all eigenvalues are real and distinct; this suffices for the case $p = q = 1$, i.e. for 2-dimensional mappings; the case of complex or multiple eigenvalues would require some modifications.)

4. The (approximate) eigenvectors of the midpoint matrix $\check{A}$, arranged in order of increasing absolute values of the corresponding eigenvalues, define the matrix Q. While Q may be computed approximately, (2) must be a rigorous enclosure of $Q^{-1}(AQ)$ for this particular Q; thus one needs to solve a linear interval equation with matrix Q and (multiple) right-hand side AQ. This choice of Q implies that in (3), the matrices B_{12} and B_{21} are nearly zero, whereas B_{11} and B_{22}^{-1} are nearly diagonal with diagonal entries less than unity. By Perron–Frobenius theory (see e.g. [16] or [3]), we can find positive vectors u, v such that $|B_{11}|u \leqslant q_1 u$ and $v^T|B_{22}^{-1}| \leqslant q_2 v$ with $q_1 \approx \lambda$ and $q_2 \approx \lambda'^{-1}$. Here the absolute value is taken componentwise.

5. We take the matrix C as an approximation of B_{22}^{-1} which implies that

$$D \approx 0, \qquad E \approx B_{22}^{-1} L B_{11}, \qquad M \approx B_{11},$$

where L is still at our disposal. Therefore, with

$$\|s\|_p := \max |s_i|/u_i, \qquad \|g\|_q := \sum |g_i| v_i,$$

we have $\|M\|_p \approx q_1$, $\|C\|_q \approx q_2$. With the choice $L = [-\alpha, \alpha] u v^T$, E is approximately contained in $[-\alpha, \alpha] q_1 q_2 u v^T = q_1 q_2 L$. Since for narrow Ω and accurate eigenvectors we can make q_1 and q_2 less than unity, one sees that (8) and (9) can always be satisfied locally. In practice, however, we may check for *any* specified Ω and α whether the closure conditions hold (without any need of approximation). If not, one can make Ω smaller and/or α larger.

6. When Σ is chosen as the box $\Sigma := [-\gamma, \gamma] u$, (10) is equivalent to $|M|u \leqslant u$, which holds locally since $|M|u \leqslant \|M\|_p u$. Condition (11) is equivalent to

$$x^* + [-\gamma, \gamma] |K| u \subseteq \Omega,$$

which can be satisfied for sufficiently small γ if $x^* \in \operatorname{int}\Omega$.

7. Once we have calculated Σ and K, (14) says that we have constructed a linear enclosure of W^s.

3.2. Transformation of linear enclosures

To verify the existence of a homoclinic point we must be able to rigorously represent pieces of the stable and unstable manifold in some neighbourhood of the homoclinic point. However, the construction of section 3.1 only yields a linear enclosure for the stable and – applied to the reverse dynamics – unstable manifold in a neighbourhood of the fixed point.

The next result shows, how these linear enclosures can be transformed to linear enclosures of the stable and unstable manifold apart from the fixed point.

Theorem 2. Let $K \in \mathbb{IR}^{n\times p}$, $x_0 \in \mathbb{IR}^n$, $t_0, \delta \in \mathbb{R}^p$, and suppose that

$$\check{x}(t_0) \in x_0, \qquad x(t) - x(s) \in K(t-s) \quad \text{for } s,t \in [t_0-\delta, t_0+\delta]. \tag{17}$$

Then $y(t) := F(x(t))$ satisfies

$$y(t_0) \in y_0 := F(\check{x}_0) + F'(x_0)(x_0 - \check{x}_0), \tag{18}$$

$$y(t) - y(s) \in H(t-s) \quad \text{for } s,t \in [t_0-\delta, t_0+\delta], \tag{19}$$

where

$$H := F'(x_e)K \quad \text{and} \quad x_e := x_0 + K[-\delta,\delta] \tag{20}$$

Moreover, the linear enclosure of the image $y(t)$ of $x(t)$ obtained in this way is not too bad: If $\operatorname{rad} x_0 = O(\|\delta\|)$, $\operatorname{rad} K = O(\|\delta\|)$, then $\operatorname{rad} y_0 = O(\|\delta\|)$, $\operatorname{rad} H = O(\|\delta\|)$, and the set of all possible $F(x(t))$ with $x(t)$ satisfying (17) has Hausdorff distance $O(\|\delta\|^2)$ from the enclosure

$$y(t) \in y_0 + H(t-t_0) \quad \text{for} \quad t \in [t_0-\delta, t_0+\delta].$$

3.3. Intersection of linear enclosures

Repeated applications of theorem 2 now allows to shift the initial enclosures of the stable and unstable manifolds into the neighbourhood of a transversal homoclinic point. The enclosure x_h of the homoclinic point is then obtained by enclosing the intersection of the two linear enclosures, which we index by s (stable) and u (unstable).

Theorem 3. Suppose that $y^s(t^s)$, $y^u(t^u)$ are continuous functions such that

$$y^s(t_0^s) \in y_0^s, \tag{21}$$

$$y^s(t) - y^s(s) \in H^s(t-s), \text{for } s,t \in [t_0^s-\delta^s, t_0^s+\delta^s], \tag{22}$$

$$y^u(t_0^u) \in y_0^u, \tag{23}$$

$$y^u(t) - y^u(s) \in H^u(t-s), \text{for } s,t \in [t_0^u-\delta^u, t_0^u+\delta^u]. \tag{24}$$

Let $z = \begin{pmatrix} x_h \\ d^s \\ d^u \end{pmatrix}$ be an enclosure of the set of solutions of the linear systems $\tilde{A}\tilde{z} = \tilde{b}$ with

$$\tilde{A} \in A := \begin{pmatrix} I & -H^s & 0 \\ I & 0 & -H^u \end{pmatrix}, \qquad \tilde{b} \in b := \begin{pmatrix} y_0^s \\ y_0^u \end{pmatrix}.$$

If A is regular and

$$|d^s| < \delta^s, \qquad |d^u| < \delta^u, \tag{25}$$

then y^s and y^u intersect transversally in a unique point

$$y^s(t^s) = y^u(t^u) \in x_h \qquad \text{with} \quad t^s \in t_0^s + d^s, t^u \in t_0^u + d^u.$$

We note that all conditions of the three theorems can be verified constructively – even in the presence of rounding errors –, using interval arithmetic with outward rounding. Their verification by a computer therefore gives a rigorous proof of the existence of a transversal homoclinic point.

In the remainder of this paper, we show the details and results of such a computer-assisted proof for a particular discrete dynamical system. For the interval calculations we used the ACRITH-XSC extension of FORTRAN77 on an IBM3090. (This package is rather slow, and we'd now rather recommend the PASCAL dialect PASCAL-XSC, available for PC's and most workstations, which has comparable interval capabilities; see Klatte et al. [11]).

4. Application to 2-dimensional mappings

4.1. Implementation of the theorems

Suppose that we have a subroutine F(N,X,Y) which calculates an interval enclosure Y of $F^N(X)$ in the interval X such that $F^N(\tilde{X}) \in Y$ for all $\tilde{X} \in X$ (if N is negative, an interval enclosure of $(F^{-1})^{-N}(X)$ is calculated). Additionally, let there be a subroutine DF(N,X,A) which calculates an interval matrix A such that $F'^N(\tilde{X}) \subseteq A$ for all $\tilde{X} \in X$. In the case of an explicit mapping, we obtain F and DF directly from the interval versions of their arithmetic expressions.

Additionally, let a variable x^* contain a (narrow) interval enclosure of a fixed point of F. If x^* is not 'known' analytically, one might run one of the various methods discussed in Neumaier [16] to obtain such an enclosure.

To test the hyperbolicity of the fixed point we call $DF(1, x^*, A)$ and calculate interval enclosures of the trace and the determinant of A,

$$\mathrm{tr}(A) = A(1,1) + A(2,2), \qquad \det(A) = A(1,1) * A(2,2) - A(1,2) * A(2,1),$$

If $\inf(\mathrm{tr}(A)^2 - 4\det(A)) \geqslant 0$ then the eigenvalues $\tilde{\lambda}_{1/2}$ and corresponding eigenvectors of all $\tilde{A} \in A$ are real and

$$\tilde{\lambda}_i \in \lambda_i = \tfrac{1}{2}\left(\mathrm{tr}(A) \pm \sqrt{\mathrm{tr}(A)^2 - 4 * \det(A)}\right), \qquad i = 1, 2.$$

If, in addition, $\pm 1 \notin \lambda_i, i = 1, 2$ then the eigenvalues $\tilde{\lambda}_{1/2}$ of all $\tilde{A} \in A$ differ from ± 1 and x^* contains a hyperbolic fixed point.

To calculate the local enclosures of $W^{u/s}$, we write a subroutine that – for a given $\Omega^{u/s} \supseteq x^*$ – calculates $K^{u/s}$ and $\Sigma^{u/s}$ such that

$$W^{u/s}(t_0) \subseteq x^* + K^{u/s} t_0 \subseteq \Omega^{u/s} \quad \text{for all } t_0 \in \Sigma^{u/s}. \tag{26}$$

In this routine we call DF(N,$\Omega^{u/s}$,A) – the sign of N determines which of the two manifolds will be enclosed –, fill Q with approximate eigenvectors of mid$A$ and calculate B by solving for the systems

of linear interval equations $QB = AQ$. With the choice $L = [-\epsilon, \epsilon]$, the narrowest enclosure of $W^{u/s}$ in Ω is given by the smallest ϵ with which the equations (7)–(9) can be satisfied. We determine this ϵ by an iterative process that results in a nearly smallest value of ϵ with which we finally calculate $K^{u/s}$ and $\Sigma^{u/s}$ from equation (5) and (10).

The implementation of theorem 2 and theorem 3 is straightforward; it is appropriate to write separate subroutines that perform these steps.

4.2. *Choosing the parameters*

Even if a mapping contains transversal homoclinic points the presented method to enclose them will fail if the six free parameters $N^{u/s}$, $t_0^{u/s}$ and $\delta^{u/s}$ are chosen badly. We therefore decribe a way of choosing and optimizing them.

As we work with linear enclosures, the curvature of W^u and W^s 'inside' the enclosures should be as little as possible to minimize the overestimation of H^u and H^s. In general, the parameters $\delta^{u/s}$ must therefore be chosen small. On the other hand, the intersection of such 'short' linear enclosures will only lead us to a valid enclosure of a transversal point of intersection x_h, if with

$$x_0^{u/s} := x^* + K^{u/s} t_0^{u/s}, \tag{27}$$

$$y_0^{u/s} := F^{N^{u/s}}(x_0^{u/s}), \tag{28}$$

the intervals $y_0^{u/s}$ are close to each other, i.e. close to the transversal homoclinic point. We achieve this by an appropriate choice of $N^{u/s}$ and $t^{u/s}$:

From calculations with finite precision arithmetic we know approximate eigenvectors $\tilde{e}^{u/s}$ of $F'(x^*)$ and the approximate location $\tilde{x}_h$ of a (suspected) homoclinic point. By calculating some images $\tilde{x}^s = F^{-N^{u/s}}(\tilde{x}_h)$ which lie in the neighbourhood of the fixed point and projecting them on $\tilde{e}^{u/s}$ we easily obtain some combinations (t_0^u, N^u) and (t_0^s, N^s) such that

$$\tilde{x}_h \approx F^{N^u}(x^* + \tilde{e}^u t_0^u) \approx F^{N^s}(x^* + \tilde{e}^s t_0^s). \tag{29}$$

We then have to decide which of these combinations is 'best'. To do this we might put $\delta^{u/s} = 0$ and for all $t_0^{u/s}$ with

$$\sigma^{u/s} = t_0^{u/s} + \delta^{u/s}, \tag{30}$$

$$\Omega^{u/s} \supseteq \begin{cases} \tilde{e}^{u/s}[0, \sigma^{u/s}] & \text{if } \sigma^{u/s} > 0, \\ \tilde{e}^{u/s}[\sigma^{u/s}, 0] & \text{if } \sigma^{u/s} < 0, \end{cases} \tag{31}$$

calculate $K^{u/s}$ according to (26) and $y_0{}^{u/s}$ from (27) and (28).

The optimal values $t_{opt}^{u/s}$ of $t_0^{u/s}$ might then be defined by

$$\diamond y_{opt}^{u/s} \leqslant \diamond y_0^{u/s} \text{ for all } t_0^{u/s}$$

where $\diamond x$ denotes the area enclosed by the interval vector x. This corresponds to the idea that we expect the best (and most secure) enclosure of x_h for those values of $t_0^{u/s}$ that gives the narrowest $y_0^{u/s}$.

Note, however, that this procedure needs quite a lot of calls of the subroutines. It is therefore of practical use only for explicit mappings, where the calculation of interval enclosure of F and F' takes

just little time. In the case of implicit mappings (e.g. Poincaré maps!), these calculations might be very time-consuming, and the choice of the 'optimal' t_0-values has then to be performed on the ground of fewer calculations, i.e. in a somewhat more heuristic way. This will be discussed in a separate paper.

Once we have selected suitable values of $t_0^{u/s}$ and $N^{u/s}$, we try to calculate an enclosure x_h of the transversal homoclinic point: First put $\delta^{u/s} = 0$, $\sigma^{u/s}$ as in (30), $\Omega^{u/s}$ as in (31), calculate $K^{u/s}$ according to (26), $y_0^{u/s}$ from (27) and (28),

$$H^{u/s} := F'^{N^{u/s}}(x_0{}^{u/s})K^{u/s} \tag{32}$$

and try to solve the system of linear interval equations

$$\begin{pmatrix} I & -H^s & 0 \\ I & 0 & -H^u \end{pmatrix} \begin{pmatrix} x_h \\ d^s \\ d^u \end{pmatrix} = \begin{pmatrix} y_0^s \\ y_0^u \end{pmatrix}. \tag{33}$$

If this is not possible, we conclude that we are not able to verify a transversal intersection of W^u and W^s in the neighbourhood of y_0^u. Otherwise we put $\delta^{u/s} > d^{u/s}$, calculate $\sigma^{u/s}$, $\Omega^{u/s}$, $K^{u/s}$, $y^{u/s}$ and $H^{u/s}$ as described above and again try to solve (33).

Now, if $\delta^{u/s} > |d^{u/s}|$ and $[t_0^{u/s} - \delta^{u/s}, t_0^{u/s} + \delta^{u/s}] \subseteq \Sigma^{u/s}$, then x_h is a valid enclosure of a transversal homoclinic point. If not, one should adjust $\delta^{u/s}$ and try again.

5. Chaos in the standard map

Let us now present some results of the application of the described method to the *reduced standard map* defined by

$$F\begin{pmatrix} q \\ p \end{pmatrix} = \begin{pmatrix} q + p - \dfrac{k}{2\pi}\sin(2\pi q) \bmod 1 \\ p - \dfrac{k}{2\pi}\sin(2\pi q) \bmod 1 \end{pmatrix}$$

which was introduced by Chirikov [4]. We have chosen it as our test mapping for the following reasons:

– The mapping is very well understood and has been the subject of several beautiful studies (e.g. [1,5,8,10,14,6]); hence it is a good test of the techniques developed in this paper.

– The mapping has one *stress parameter* k by which the 'amount of nonlinearity' can easily be tuned such that the mapping is linear for $k = 0$ and becomes more and more nonlinear with increasing values of $k > 0$. Numerical simulations and theoretical considerations suggest that the mapping is chaotic for all $k > 0$; indeed, the existence of chaotic trajectiories has been proved rigorously for $k > 6.86$ (Aubry and Abramovici [1]), and the absense of rotational invariant circles (an indication of widespread chaos) was proved rigorously for $k > 63/64$ by MacKay and Percival [15].
The latter paper uses (implicitly) interval arithmetic and linear enclosures, but on a more elementary level.

– To the best of our knowledge, the existence of transversal homoclinic points has never been proved rigorously. We establish their existence for $k = 1.5$ and $k = 0.23$, the latter value being much below the onset of widespread chaos believed to begin at $k = 0.971635$ (Greene [8]).

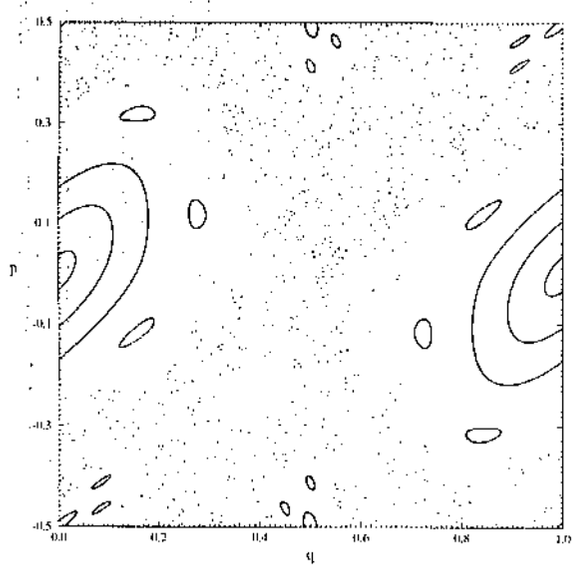

Fig. 3. Phase portrait of the standard map at $k = 3/2$.

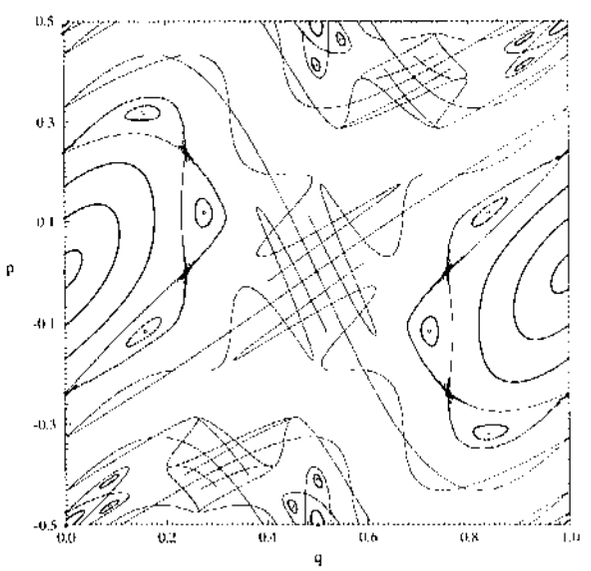

Fig. 4. Modified phase portrait of the standard map at $k = 3/2$.

– To apply the theory of the previous sections, the mapping has to be a diffeomorphism and we need its inverse F^{-1} and the stability matrices F' and $(F^{-1})'$ of F and F^{-1}. For the standard map, these can easily be calculated and no problems occur in calculating their interval extensions as well. In particular we find

$$F^{-1}\begin{pmatrix} q \\ p \end{pmatrix} = \begin{pmatrix} q - p \bmod 1 \\ p + \dfrac{k}{2\pi}\sin(2\pi(q-p)) \bmod 1 \end{pmatrix}, \quad F'\begin{pmatrix} q \\ p \end{pmatrix} = \begin{pmatrix} 1 - k\cos(2\pi q) & 1 \\ -k\cos(2\pi q) & 1 \end{pmatrix},$$

$$(F^{-1})'\begin{pmatrix} q \\ p \end{pmatrix} = \begin{pmatrix} 1 & -1 \\ k\cos(2\pi(q-p)) & 1 - k\cos(2\pi(q-p)) \end{pmatrix}.$$

As $\det F' = 1$, the mapping F is area preserving.

– For every value of k there is a fixed point at $(q^*, p^*) = (\frac{1}{2}, 0)$ which can easily shown to be hyperbolic for $0 < k < 4$.

In fig. 3 we show a kind of portrait of the standard map at the value of $k = \frac{3}{2}$. Here we have plotted 1000 iterations (calculated with double precision arithmetic) of each of 7 different, carefully chosen, starting points. We see islands of stability for some elliptic fixed points (of order $n = 1, 2, 4, 6$ and 8) embedded in a 'sea of chaos'. Indeed, the random-like pattern is the repeated image of only one single starting point close to the center of the picture.

Fig. 4 helps us to understand the mechanism of chaos. Here, we have replaced the chaotic orbit of fig. 3 by approximately computing pieces of the stable and unstable manifolds of some hyperbolic fixed points (of order $n = 1, 2, 4, 6$ and 8). The figure contains several invariant closed curves and several parts of manifolds associated with hyperbolic fixed points.

The invariant closed curves were obtained by selecting interactively an appropriate starting point and iterating it with F until the curve was uniformly covered to drawing accuracy. The unstable

manifolds were obtained as follows:

First we calculated the location of a fixed point close to an interactively selected point, using Newton's method, and calculated the eigenvectors of the Jacobian at this point. In a neighbourhood of the fixed point we selected a fixed number of closely spaced points covering a piece of the line through the fixed point along the unstable eigenvector, not including the fixed point itself. Iterating this set of points with F yields points lying approximately on the unstable manifold. Whenever the distance of the points became so large that gaps in the curve appeared, part of the points in the most recent iterated set were replaced by points obtained from linear interpolation of adjacent points. Finally, the manifolds were cut off interactively.

The stable manifolds were obtained in the same way by using F^{-1} instead. All necessary calculations were performed with double precision arithmetic. (For algorithms to calculate invariant manifolds, see also Parker and Chua [17]).

As we detect quite a lot of transversal crossings of the various manifolds, these 'approximate pictures' give strong evidence of chaos in the standard map, and from the practical point of view, this is fully sufficient. However, from a mathematical point of view we have to make sure that these transversal crossings are not artefacts produced by rounding errors; so we have to run our method to enclose at least one of them.

Let us first concentrate on the transversal point at $\tilde{x}_h = (0.328, 0.328)$. Using the approximate eigenpair

$$\tilde{\lambda}^u = 3.1861, \qquad \tilde{e}^u = \begin{pmatrix} 0.8246 \\ 0.5658 \end{pmatrix},$$

we list in table 1 some values of N^u and t_0^u that satisfy (29). For each t_0^u we also present the corresponding values of $\diamond K^u$, $\diamond x_0^u$ and $\diamond y_0^u$ as they are obtained by our method with $\delta^u = 0$ and Ω^u chosen according to (30) and (31).

For $N^u < 17$ one sees that $\diamond K^u$ decreases quadratically with increasing N^u. This confirms the quadratic approximation property of our method to enclose stable manifolds. The fact that $\diamond K^u$ does not converge towards zero but to a positive value is due to the fact that we are working with finite precision (interval) arithmetic that defines a limit of accuracy. As expected, $\diamond x_0^u$ initially decreases in third order, but again, the finite precision limits this dependence for $N^u > 16$ and $\diamond x_0^u$ converges towards a nonzero value.

$\diamond y_0^u$ shows a quadratic convergence property as long as $N^u < 11$. For $N^u > 11$ the behaviour of $\diamond y_0^u$ is governed by the fact that we are working with an interval enclosure

$$[\underline{\pi}, \overline{\pi}] = [\,3.1415926535897931\,, 3.1415926535897936\,]$$

of π such that for $N^u > 11$ the value of $\diamond F(x_0^u)$ is not dependent on $\diamond x_0^u$ any longer but on $\mathrm{rad}[\underline{\pi}, \overline{\pi}] = 2.5\ \mathrm{e}{-16}$. Therefore $\diamond y_0^u$ increases almost linearly for $N^u > 13$ with $\diamond y_0^u(N^u + 1)/\diamond y_0^u(N^u)$ being approximately equal to the average blowup

$$\Delta(x) = \frac{\diamond F(x)}{\diamond x} \approx 10$$

of the area of an interval under one application of F.

As $\diamond y_0^u$ takes its minimum at $N^u = 12$, the combination $N^u = 12$, $t_0^u = 1.9542\ \mathrm{e}{-06}$ is the best choice for these two parameters. In the same way, we find the optimal combination of N^s and t_0^s to be $N^s = -10$, $t_0^s = 3.8737\ \mathrm{e}{-06}$.

Table 1
Some (N^u, t_0^u)-combinations to 'reach' the transversal homoclinic point $\tilde{x}_h = (0.328, 0.328)$ of the standard map at $k = 3/2$.

N^u	t_0^u	$\diamond K^u$	$\diamond x_0^u$	$\diamond y_0^u$
5	6.5135 e−03	4.5 e−08	1.9 e−12	2.6 e−08
6	2.0444 e−03	4.4 e−10	1.8 e−15	2.5 e−10
7	6.4164 e−04	4.3 e−12	1.8 e−18	2.4 e−12
8	2.0139 e−04	4.1 e−14	1.7 e−21	2.3 e−14
9	6.3207 e−05	4.0 e−16	1.6 e−24	2.3 e−16
10	1.9838 e−05	3.9 e−18	1.5 e−27	2.2 e−18
11	6.2263 e−06	3.8 e−20	1.5 e−30	2.5 e−20
12	1.9542 e−06	3.7 e−22	2.3 e−33	2.8 e−21
13	6.1334 e−07	3.6 e−24	2.4 e−35	1.6 e−20
14	1.9250 e−07	3.5 e−26	7.3 e−37	1.7 e−19
15	6.0419 e−08	3.4 e−28	2.3 e−38	1.6 e−18
16	1.8963 e−08	3.5 e−30	7.3 e−40	1.6 e−17
17	5.9517 e−09	1.0 e−31	4.0 e−41	1.7 e−16
18	1.8680 e−09	1.4 e−32	5.0 e−42	1.8 e−15
19	5.8629 e−10	1.4 e−32	2.2 e−42	1.7 e−14
20	1.8401 e−10	1.4 e−32	5.0 e−43	1.8 e−13

Table 2
Results of the enclosure of the transversal homoclinic point $x_h \approx (0.328, 0.328)$ of the the standard map at $k = 3/2$ for different $\delta^u = \delta^s = \delta$.
$(N^u = 12,\ t_0^u = 1.9542\ \text{e}{-06},\ N^s = 10,\ t_0^s = 3.8737\ \text{e}{-06})$

δ	$\diamond H^u$	$\diamond H^s$	$\lvert d^u \rvert$	$\lvert d^s \rvert$	$\diamond x_h$
1.00 e−17	1.05 e−09	2.42 e−12	4.36 e−16	6.70 e−16	4.55 e−21
1.00 e−15	8.51 e−08	7.73 e−10	4.36 e−16	6.70 e−16	4.55 e−21
1.00 e−13	6.87 e−04	4.74 e−07	4.36 e−16	6.70 e−16	4.55 e−21
1.00 e−11	6.86 e+00	4.71 e−03	4.36 e−16	6.70 e−16	4.55 e−21
1.00 e−09	6.87 e+04	4.71 e+01	4.37 e−16	6.71 e−16	4.57 e−21
1.00 e−07	8.39 e+08	4.72 e+05	6.33 e−16	9.53 e−16	1.02 e−20
3.00 e−07	1.08 e+10	4.25 e+06	3.08 e−14	5.09 e−14	3.03 e−17
3.05 e−07	1.13 e+10	4.40 e+07	1.48 e−13	2.48 e−13	7.05 e−16
3.07 e−07	1.14 e+10	4.45 e+06	1.17 e−12	1.98 e−11	4.43 e−14
3.08 e−07	1.15 e+10	4.48 e+06	–	–	–

In the next step we have to choose the parameters δ^u and δ^s. In Table 2 we list the obtained values of $\diamond H^u$, $\diamond H^s$, $|d^u|$ and $|d^s|$ that we obtain by putting $\delta^u = \delta^s = \delta$.

Note that for $\delta \leqslant 1$ e−09 the obtained values of $|d^{u/s}|$ and $\diamond x_h$ are independent of the 'length' δ of the linear enclosures. For $\delta \geqslant 1$ e−07 all three quantities increase exponentially with increasing δ, showing that the matrix A of the linear system of interval equations becomes more and more

Table 3
Results of the enclosure of transversal homoclinic points in the standard map for different values of k.

k	N^u	t_0^u	δ^u	N^s	t_0^s	δ^s	$\diamond x_h$
1.50	10	1.95419 e−06	2.84 e−16	12	3.87371 e−06	4.12 e−16	1.35 e−21
1.00	11	2.47791 e−06	7.31 e−16	15	4.00934 e−06	1.01 e−15	1.38 e−21
0.80	12	1.51305 e−06	1.50 e−15	18	2.23054 e−06	1.19 e−15	3.91 e−21
0.70	13	2.22329 e−06	2.65 e−15	18	3.11983 e−06	3.81 e−15	1.79 e−20
0.60	13	1.74876 e−06	3.66 e−15	21	2.33168 e−06	4.72 e−15	7.41 e−21
0.50	14	1.80895 e−06	1.18 e−14	23	-2.28816 e−06	1.50 e−14	5.90 e−20
0.40	14	1.92473 e−06	5.97 e−14	27	-2.30717 e−06	5.33 e−14	2.01 e−19
0.30	15	1.52470 e−06	3.18 e−13	33	-1.73178 e−06	3.61 e−13	1.61 e−18
0.25	14	2.18948 e−06	2.5d e−12	38	-1.47644 e−06	1.52 e−11	9.19 e−17
0.23	14	1.77710 e−06	6.13 e−12	40	-1.94548 e−06	6.71 e−11	2.87 e−16
0.20	14	1.70980 e−06	–	44	-1.84346 e−06	–	–

ill-conditioned. (For $\delta \geqslant 3.08$ e−07 the matrix is numerically singular, and the system of interval equations can no longer be solved.)

To obtain a valid enclosure x_h of a transversal homoclinic point, we must choose δ^u and δ^s such that $|d^{u/s}| < \delta^{u/s}$. These conditions are satisfied with $\delta^u = 5$ e−16 and $\delta^s = 7$ e−16. The enclosure x_h of the transversal homoclinic point obtained with these values reads

$$x_h \subset \begin{pmatrix} [\,0.328060679327\,,0.328060679380\,] \\ [\,0.328060679309\,,0.328060679398\,] \end{pmatrix}.$$

With respect to the application of this method to other mappings, it is important to know how 'obvious' the presence of transversal homoclinic points must be in order to be able to rigorously enclose them, i.e. what percentage of phase space must be 'occupied' by the broken separatrix. We therefore list in Table 3 the results of the method for different values of the stress parameter k. For each k-value we present the 'optimal' values of N^u, t_0^u, δ^u, N^s, t_0^s und δ^s and the obtained area $\diamond x_h$ of the enclosure of a transversal homoclinic point.

Note that at $k = 1.5$, with t_0^u and t_0^s as given above but $N^u = 10$ and $N^s = -12$ (corresponding to the homoclinic point $\tilde{x}_h \approx (0.672, 0.118)$), we obtain an enclosure x_h with area $\diamond x_h = 1.35$ e−21. This result is listed in Table 3 as it is the narrowest enclosure we were able to compute at $k = 3/2$.

Figure 5 shows a phase portrait of the standard map at $k = 0.23$, the lowest values of k at which we were able to enclose a transversal homoclinic point. (For comparison: Grebogi et al. [6] give results for rigorously shadowing a chaotic orbit of the standard map down to $k = 0.97$, and MacKay and Percival's converse KAM technique [15] starts to fail slightly above $k = 0.97$.) One sees the islands of stability of the elliptic fixed points of order $n = 1$ and 2 and some invariant tori that divide the phase space. Additionally we have plotted pieces of the stable and unstable manifold of the hyperbolic fixed point $x^* = (0.5, 0)$.

At the right side of the picture you find two successive magnifications of phase space around x^*. From these blow-ups, we conclude that the existence of transversal homoclinic points in the standard map can be rigorously proved even if the broken separatrix occupies just about a millionth of the total

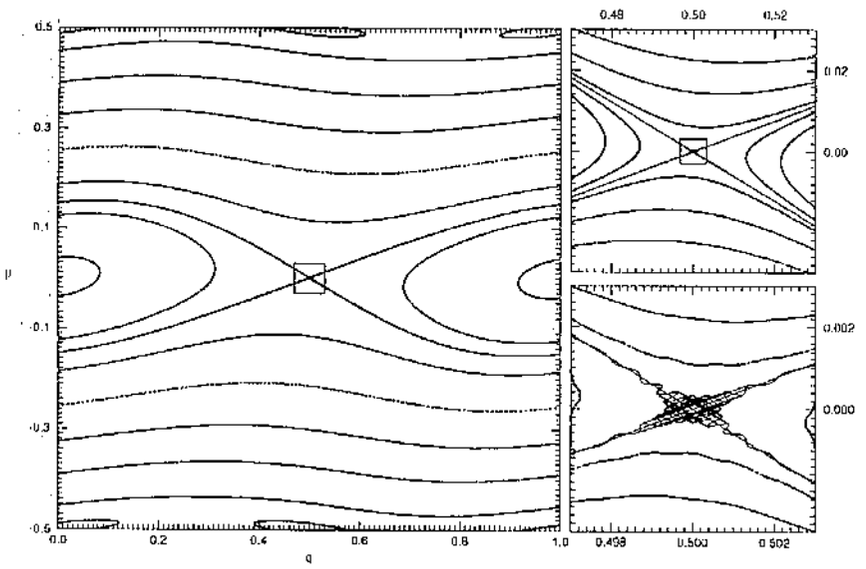

Fig. 5. Phase portraits of the standard map at $k = 0.23$.

volume of phase space.

6. Proofs

Proof of theorem 1. We establish that the functional equation (12) has a solution $x(t)$ of the form (13), where $g(t)$ satisfies (15). By inserting (13) into (12) and multiplying by $(I,0)Q^{-1}$ we see that this requires

$$\sigma(t) = (I,0)Q^{-1}[F(x(t)) - F(x^*)], \tag{34}$$

and we shall take this as the definition of $\sigma(t)$. Multipling (12) by $(0,I)Q^{-1}$ we find the additional condition

$$g(\sigma(t)) = (0,I)Q^{-1}[F(x(t)) - F(x^*)]. \tag{35}$$

Clearly, (34) and (35) together imply (12); hence it suffices to solve (35) for $g(t)$, with $x(t)$ expressed in terms of $g(t)$ by (13). We shall do this by an application of the fixed point theorem of Banach to the nonlinear operator Φ which maps a function g to the function $\Phi(g) := \overline{g}$ defined by

$$\overline{g}(t) := g(t) + C\left[g(\sigma(t)) - (0,I)Q^{-1}\left(F(x(t)) - F(x^*)\right)\right]. \tag{36}$$

Since C is assumed nonsingular, a fixed point of Φ is indeed a solution of (35).

We now come to the main part of the proof, which consists in showing that Φ is a contraction on the set K of all functions $g : \Sigma \to \mathbb{R}^q$ satisfying (15). This will be done in four stages: We show that
(i) Φ is well-defined on K,
(ii) Φ maps K into K,
(iii) K is a closed subset of a suitable Banach space V, and

(iv) Φ is Lipschitz continuous with Lipschitz constant < 1.

Then Banach's fixed point theorem guarantees the existence of a unique fixed point of Φ, which proves the theorem.

(i) To show that Φ is well-defined on K we choose some function $g \in K$. Thus g satisfies (15), i.e., we can find some matrix $\tilde{L} \in L$ such that

$$g(t) - g(s) = \tilde{L}(t-s). \tag{37}$$

In general, $\tilde{L}$ depends on t and s. In particular, since $g(0) = 0$ we find $g(t) = \tilde{L}t$, hence (11) and (13) yield

$$x(t) = x^* + Q\begin{pmatrix} t \\ \tilde{L}t \end{pmatrix} = x^* + Q\begin{pmatrix} I \\ \tilde{L} \end{pmatrix} \in x^* + Kt \subseteq \Omega \quad \text{for all } t \in \Sigma.$$

Thus condition (11) is instrumental for restricting $x(t)$ to the domain of F. Now we can apply (2) and find a matrix $\tilde{A} \in A$ such that

$$F(x(t)) - F(x(s)) = \tilde{A}(x(t) - x(s)),$$

where, again, $\tilde{A}$ depends on t and s. Using (13) and (37), we obtain

$$Q^{-1}[F(x(t)) - F(x(s))] = Q^{-1}\tilde{A}Q\begin{pmatrix} t-s \\ g(t)-g(s) \end{pmatrix} = Q^{-1}\tilde{A}Q\begin{pmatrix} t-s \\ \tilde{L}(t-s) \end{pmatrix}.$$

By (3), we can write

$$Q^{-1}\tilde{A}Q = \begin{pmatrix} \widetilde{B_{11}} & \widetilde{B_{12}} \\ \widetilde{B_{21}} & \widetilde{B_{22}} \end{pmatrix}$$

with $\tilde{B}_{ik} \in B_{ik}$; hence we obtain

$$Q^{-1}[F(x(t)) - F(x(s))] = \begin{pmatrix} (\tilde{B}_{11} + \tilde{B}_{12}\tilde{L})(t-s) \\ (\tilde{B}_{21} + \tilde{B}_{22}\tilde{L})(t-s) \end{pmatrix} = \begin{pmatrix} \widetilde{M} \\ \tilde{N} \end{pmatrix}(t-s), \tag{38}$$

where, using (7),

$$\widetilde{M} = \tilde{B}_{11} + \tilde{B}_{12}\tilde{L} \in M, \tilde{N} = \tilde{B}_{21} + \tilde{B}_{22}\tilde{L}. \tag{39}$$

(34) now yields

$$\sigma(t) - \sigma(s) = (I, 0)\,Q^{-1}[F(x(t)) - F(x(s))] = \widetilde{M}(t-s), \tag{40}$$

proving (16). In particular, since $\sigma(0) = 0$ by (34), we get

$$\sigma(t) \in Mt. \tag{41}$$

Thus we see that condition (10) serves to guarantee that $\{\sigma(t) | t \in \Sigma\} \subseteq \Sigma$. This shows that $g(\sigma(t))$ is well-defined for $t \in \Sigma$, and (36) then yields a well-defined $\overline{g}(t)$. Thus $\overline{g} = \Phi(g)$ is well defined.

(ii) To show that Φ maps K onto itself we have to show that $\overline{g}$ also satisfies (15). Now (36) gives $\overline{g}(0) = g(0) + Cg(\sigma(0)) = 0$ since $g(0) = 0$ and $\sigma(0) = 0$. Again by (36), we have

$$\overline{g}(t) - \overline{g}(s) = g(t) - g(s) + C[g(\sigma(t)) - g(\sigma(s)) - (0, I)\, Q^{-1}(F(x(t)) - F(x(s)))].$$

We employ (37)–(40) to reduce this (for suitable $\widetilde{L}' \in L$) to

$$\begin{aligned}\overline{g}(t) - \overline{g}(s) &= \widetilde{L}(t-s) + C[\,\widetilde{L}'(\sigma(t) - \sigma(s)) - \widetilde{N}(t-s)\,] \\ &= \widetilde{L}(t-s) + C[\,\widetilde{L}'\widetilde{M}(t-s) - \widetilde{N}(t-s)\,] = \overline{L}(t-s)\end{aligned} \tag{42}$$

with the matrix

$$\begin{aligned}\overline{L} &= \widetilde{L} + C(\widetilde{L}'\widetilde{M} - \widetilde{N}) = \widetilde{L} + C\,\widetilde{L}'(\widetilde{B}_{11} + \widetilde{B}_{12}\widetilde{L}) - C\,(\widetilde{B}_{21} + \widetilde{B}_{22}\,\widetilde{L}) \\ &= [I + C\,(\widetilde{L}'\widetilde{B}_{12} - \widetilde{B}_{22})]\widetilde{L}C\,(\widetilde{L}'\widetilde{B}_{11} - \widetilde{B}_{21}) \in D\widetilde{L} + E \subseteq DL + E \subseteq L.\end{aligned}$$

by (9). Thus the condition (9) serves to force $\overline{L} \in L$, and together with (42) this establishes that $\overline{g} \in K$. Thus Φ maps K into itself.

(iii) We consider the space of all continuous functions with finite norm

$$\|g\| := \sup_{t \in \Sigma \setminus \{0\}} \frac{\|g(t)\|}{\|t\|}. \tag{43}$$

This space is easily seen to be a Banach space V. Now V contains K since (15) implies (for $s = 0$) that

$$\|g\| \leqslant \|L\|.$$

To show that K is closed we consider a sequence of functions $g_l \in K$ $(l = 0, 1, \ldots)$ with limit g. Then

$$\|g(t) - g_l(t)\| \leqslant \|g - g_l\|\|t\| \text{for all} t \in \Sigma,$$

hence

$$\|(g(s) - g(t)) - (g_l(s) - g_l(t))\| \leqslant \|g - g_l\|(\|s\| + \|t\|).$$

With some interval vector b enclosing the unit ball in $\mathbb{R}^q$, this yields

$$g(s) - g(t) \in g_l(s) - g_l(t) + \|g - g_l\|\,(\|s\| + \|t\|)\, b \subseteq L(s-t) + \|g - g_l\|\,(\|s\| + \|t\|)\, b;$$

In the limit $l \to \infty$ we obtain

$$g(s) - g(t) \in L(s-t).$$

Since obviously $g(0) = 0$, this shows that $g \in K$. Therefore K is closed.

(iv) To show that Φ is Lipschitz continuous we consider two functions $g_1, g_2 \in K$ and the corresponding functions $x = x_i$ and $\sigma = \sigma_i$ defined by (13) and (34) for $g = g_i$ $(i = 1, 2)$. We can find matrices $\widetilde{A} \in A$ and $\widetilde{B}_{ik} \in B_{ik}$, with $\widetilde{A}$ different from that in (i), such that

$$\begin{aligned}&Q^{-1}\,[\,F(x_1(t)) - F(x_2(t))\,] = Q^{-1}\,\widetilde{A}\,(x_1(t) - x_2(t)) \\ &= Q^{-1}\,\widetilde{A}\,Q \begin{pmatrix} 0 \\ g_1(t) - g_2(t) \end{pmatrix} = \begin{pmatrix} \widetilde{B}_{12}(g_1(t) - g_2(t)) \\ \widetilde{B}_{22}(g_1(t) - g_2(t)) \end{pmatrix}.\end{aligned} \tag{44}$$

In particular

$$\sigma_1(t) - \sigma_2(t) = \tilde{B}_{12}(g_1(t) - g_2(t)).$$

We can also find a matrix $\tilde{L} \in L$, different from that in (i), such that

$$g_2(\sigma_1(t)) - g_2(\sigma_2(t)) = \tilde{L}(\sigma_1(t) - \sigma_2(t)) = \tilde{L}\tilde{B}_{12}(g_1(t) - g_2(t)). \tag{45}$$

Hence the functions $\overline{g}_i = \Phi(g_i)$ satisfy

$$\begin{aligned}\overline{g_1}(t) - \overline{g_2}(t) &= g_1(t) - g_2(t) + C[g_1(\sigma_1(t)) - g_2(\sigma_2(t))] - C(0, I)Q^{-1}[F(x_1(t)) - F(x_2(t))] \\ &= g_1(t) - g_2(t) + C[g_1(\sigma_1(t)) - g_2(\sigma_1(t)) + \tilde{L}\tilde{B}_{12}(g_1(t) - g_2(t))] - C\tilde{B}_{22}(g_1(t) - g_2(t)) \\ &= \tilde{D}(g_1(t) - g_2(t)) + C[g_1(\sigma_1(t)) - g_2(\sigma_1(t))],\end{aligned}$$

where $\tilde{D} = I + C(\tilde{L}\tilde{B}_{12} - \tilde{B}_{22}) \in D$ by (4). Using (41) and (43), we find

$$\begin{aligned}\|\overline{g_1}(t) - \overline{g_2}(t)\| &\leq \|D\|\|g_1 - g_2\|\|t\| + \|C\|\|g_1 - g_2\|\|\sigma_1(t)\| \\ &\leq \|D\|\|g_1 - g_2\|\|t\| + \|C\|\|g_1 - g_2\|\|M\|\|t\| = (\|D\| + \|C\|\|M\|)\|g_1 - g_2\|\|t\|,\end{aligned}$$

and therefore

$$\|\Phi(g_1) - \Phi(g_2)\| = \|\overline{g_1} - \overline{g_2}\| \leq (\|D\| + \|C\|\|M\|)\|g_1 - g_2\|.$$

Thus Φ is Lipschitz continuous with Lipschitz constant $\|D\| + \|C\|\|M\|$, and condition (8) serves to force this Lipschitz constant to be < 1. □

Proof of theorem 2. (18) holds by Neumaier [16], theorem 2.3.3 since y_0 is a centered form for the range of $f(\tilde{x})$, $\tilde{x} \in x_0$. To prove (19) we note that the assumption implies $x(t) - x(s) = \tilde{K}(t - s)$ with $\tilde{K} \in K$, hence by the mean value theorem, the components of $y(t)$ satisfy

$$y_i(t) - y_i(s) = f_i(x(t)) - f_i(x(s)) = f_i'(\xi_i)(x(t) - x(s)) = f_i'(\xi_i)\tilde{K}(t - s),$$

with suitable $\xi_i \in \square\{x(t), x(s)\} \subseteq x_e$ by (17). Hence $f_i'(\xi_i)\tilde{K}$ lies in $f_i'(x_e)K$, the i-th row of H, so that

$$y(t) - y(s) \in (f'(x_e)K)(t - s) = H(t - s).$$

Finally, the asymptotic results follow from the quadratic approximation property of the centered form (Neumaier [16], theorem 2.3.3.). □

Proof of theorem 3. Let x^0 be a box which contains x in its interior. We define a function

$$G : x^0 \times [t_0^s - \delta^s, t_0^s + \delta^s] \times [t_0^u - \delta^u, t_0^u + \delta^u] \to \mathbb{R}^{2n}$$

by

$$G(\tilde{x}, t^s, t^u) := \begin{pmatrix} \tilde{x} - y^s(t^s) \\ \tilde{x} - y^u(t^u) \end{pmatrix}.$$

The assumptions imply that

$$-G(0, t_0^s, t_0^u) = \begin{pmatrix} y^s(t_0^s) \\ y^u(t_0^u) \end{pmatrix} =: \tilde{b} \in b,$$

$$G(\tilde{x}, t^s, t^u) - G(\tilde{x}', t^{s\prime}, t^{u\prime}) = \begin{pmatrix} \tilde{x} - \tilde{x}' - \widetilde{K^s}(t^s - t^{s\prime}) \\ \tilde{x} - \tilde{x}' - \widetilde{K^u}(t^u - t^{u\prime}) \end{pmatrix}. \tag{46}$$

for suitable $\widetilde{K^s} \in K^s$, $\widetilde{K^u} \in K^u$. The right hand side of (46) can be written as

$$\begin{pmatrix} I & -\widetilde{K^s} & 0 \\ I & 0 & -\widetilde{K^u} \end{pmatrix} \begin{pmatrix} \tilde{x} - \tilde{x}' \\ t^s - t^{s\prime} \\ t^u - t^{u\prime} \end{pmatrix} \in A \left(\begin{pmatrix} \tilde{x} \\ t^s \\ t^u \end{pmatrix} - \begin{pmatrix} \tilde{x}' \\ t^{s\prime} \\ t^{u\prime} \end{pmatrix} \right);$$

hence A is a Lipschitz matrix for G. Therefore, theorem 5.1.7 (iii) of Neumaier [16] applies and shows the existence of a unique solution of the system $G(\tilde{x}, t^s, t^u) = 0$ with

$$\begin{pmatrix} \tilde{x} \\ t^s \\ t^u \end{pmatrix} \in \begin{pmatrix} 0 \\ t_0^s \\ t_0^u \end{pmatrix} - A^H G(0, t_0^s, t_0^u) \subseteq \begin{pmatrix} 0 \\ t_0^s \\ t_0^u \end{pmatrix} + z = \begin{pmatrix} x \\ t_0^s + d^s \\ t_0^u + d^u \end{pmatrix}.$$

It remains to show that the manifolds y^s and y^u intersect transversally. This means that the tangent spaces of y^s and y^u span the whole space, i.e. the matrix

$$\left(\frac{\mathrm{d}y^s}{\mathrm{d}t^s}(t^s), \frac{\mathrm{d}y^u}{\mathrm{d}t^u}(t^u) \right) \tag{47}$$

must be shown to be nonsingular. But the Lipschitz conditions (22) and (24) imply (for $s, t \to t^s$ resp. t^u) that

$$\widetilde{K^s} := \frac{\mathrm{d}y^s}{\mathrm{d}t^s}(t^s) \in K^s, \widetilde{K^u} := \frac{\mathrm{d}y^u}{\mathrm{d}t^u}(t^u) \in K^u.$$

Now any solution of $(\widetilde{K^s}, \widetilde{K^u})\binom{p}{q} = 0$ satisfies $\widetilde{K^s}p = -\widetilde{K^u}q =: \overline{x}$, hence

$$A \begin{pmatrix} \overline{x} \\ p \\ -q \end{pmatrix} = \begin{pmatrix} I & -K^s & 0 \\ I & 0 & -K^u \end{pmatrix} \begin{pmatrix} \overline{x} \\ p \\ -q \end{pmatrix} = \begin{pmatrix} \overline{x} - K^s p \\ \overline{x} + K^u q \end{pmatrix} \ni 0.$$

Since A is regular, this forces $\overline{x} = 0$, $p = 0$, $q = 0$ ([16], Corollary 3.4.5). Therefore the matrix $(\widetilde{K^s}, \widetilde{K^u})$, i.e. (47), has only a trivial null space, and hence is nonsingular. Thus y^s and y^u intersect transversally. □

7. Conclusions

In the preceding sections we have described a computer-assisted proof for the rigorous verification of the existence of transversal homoclinic points in 2-dimensional discrete dynamical systems. We also discussed briefly the relation between such points and deterministic chaos.

The results of the application of the method to the standard map suggest that it is applicable as well to a lot of other explicit and implicit mappings. Indeed, we have already successfully applied it to a Poincaré map of the so-called Thiele–Wilson system and will publish these results in a later article.

Clearly, our method is not restricted to conservative systems (such as the standard map); only the invertibility of the mapping F is needed. The method also applies to higher-dimensional systems provided the eigenvalues of the Jacobian at the hyperbolic fixed point in question are all real and distinct. With just a few modifications, the method also allows the rigorous verification of transversal *heteroclinic* points.

We conclude that interval analysis is a useful mathematical tool to obtain rigorous validations of statements obtained approximately by numerical simulations of dynamical systems.

Acknowledgments

We gratefully acknowledge the support by Prof. Christoph Schlier who suggested the problem and supplied us with the computing facilities, and by Ansgar Seiter who provided software for approximate chaos calculations.

References

[1] S. Aubry and G. Abramovici, Chaotic trajectories in the standard map, the concept of anti-integrability, Physica D 43 (1990) 199–219.
[2] F. Battelli and K.J. Palmer, Chaos in the Duffing equation, J. Diff. Equations 101 (1993) 276–301.
[3] A. Berman and R.J. Plemmons, Nonnegative Matrices in the Mathematical Sciences (Academic Press, New York, 1979).
[4] B.V. Chirikov, A universal instability of many-dimensional oscillator systems, Phys. Rep. 52 (1979) 263–379
[5] J.D.J. Earn, Exact numerical studies of hamiltonian maps: iterating without roundoff error, Physica D 56 (1992) 1–22.
[6] C. Grebogi, S.M. Hammel, J.A. Yorke and T. Sauer, Shadowing of physical trajectories in chaotic dynamics, containment and refinement, Phys. Rev. Lett. 65 (1990) 1527–1530.
[7] S.M. Hammel, J.A. Yorke, C. Grebogi, Bull. Amer. Math. Soc. 19 (1988) 465–469.
[8] J.M. Greene, A method for determining a stochastic transition, J. Math. Phys. 20 (1979) 1183–1201.
[9] P. Hartman, Ordinary Differential Equations (Wiley, New York, 1964).
[10] J.M. Ketoja and R.S. MacKay, Fractal boundary for the existence of invariant circles for area preserving maps: observations and renormalization explanation, Physica D 35 (1989) 318–334.
[11] R. Klatte et al., PASCAL-XSC Language Reference with Examples (Springer, Berlin, 1992).
[12] F.R. Marotto, Chaotic behaviour in the Hénon mapping, Commun. Math. Phys. 68 (1979) 187–194.
[13] T. Matsumoto, L.O. Chua and T. Lin, Reality of chaos in the double scroll circuit, IEEE Transactions on Circuits and Systems, 35 (1988) 909.
[14] R.S. MacKay, J.D. Meiss and I.C. Percival, Resonances in area preserving maps, Physica D 27 (1987) 1–20.
[15] R.S. MacKay and I.C. Percival, Converse KAM: theory and practice, Commun. Math. Phys. 98 (1985) 469–512.
[16] A. Neumaier, Interval Methods for Systems of Equations (Cambridge Univ. Press, Cambridge, 1990).
[17] T.S. Parker und L.O. Chua; Practical Numerical Algorithms for Chaotic Systems (Springer Verlag, Berlin, 1989).
[18] S. Smale, Differentiable dynamical systems, Bull. Amer. Math. Soc. 73 (1967) 747–817.
[19] M. Tabor, Chaos and Integrability in Nonlinear Dynamics (Wiley, New York, 1989).
[20] S. Wiggins, On the geometry of transport in phase space, Physica D 44 (1990) 471–501.